PHYSICAL REVIEW E **83**, 056309 (2011)

Transport coefficients for the shear dynamo problem at small Reynolds numbers

Nishant K. Singh[1,2,*] and S. Sridhar[1,†]
[1]*Raman Research Institute, Sadashivanagar, Bangalore 560 080, India*
[2]*Joint Astronomy Programme, Indian Institute of Science, Bangalore 560 012, India*
(Received 14 March 2010; revised manuscript received 5 March 2011; published 9 May 2011)

We build on the formulation developed in S. Sridhar and N. K. Singh [J. Fluid Mech. **664**, 265 (2010)] and present a theory of the *shear dynamo problem* for small magnetic and fluid Reynolds numbers, but for arbitrary values of the shear parameter. Specializing to the case of a mean magnetic field that is slowly varying in time, explicit expressions for the transport coefficients α_{il} and η_{iml} are derived. We prove that when the velocity field is nonhelical, the transport coefficient α_{il} vanishes. We then consider forced, stochastic dynamics for the incompressible velocity field at low Reynolds number. An exact, explicit solution for the velocity field is derived, and the velocity spectrum tensor is calculated in terms of the Galilean-invariant forcing statistics. We consider forcing statistics that are nonhelical, isotropic, and delta correlated in time, and specialize to the case when the mean field is a function only of the spatial coordinate X_3 and time τ; this reduction is necessary for comparison with the numerical experiments of A. Brandenburg, K. H. Rädler, M. Rheinhardt, and P. J. Käpylä [Astrophys. J. **676**, 740 (2008)]. Explicit expressions are derived for all four components of the magnetic diffusivity tensor $\eta_{ij}(\tau)$. These are used to prove that the shear-current effect cannot be responsible for dynamo action at small Re and Rm, but for all values of the shear parameter.

DOI: 10.1103/PhysRevE.83.056309 PACS number(s): 47.27.W−, 47.65.Md, 52.30.Cv, 95.30.Qd

I. INTRODUCTION

Astrophysical systems such as planets, galaxies, and clusters of galaxies possess magnetic fields which exhibit definite spatial ordering, in addition to a random component. The ordered (or "large scale") components are thought to originate from turbulent dynamo action in the electrically conducting fluids in these objects. The standard model of such a process involves amplification of seed magnetic fields due to turbulent flows which lack mirror symmetry (equivalently, which possess helicity) [1–3]. The turbulent flows generally possess large-scale shear, which is expected to have significant effects on transport properties [4]; however, it is not clear whether the turbulent flows are always helical. Recent work has explored the possibility that nonhelical turbulence in conjunction with background shear may give rise to large-scale dynamo action [5–10]. The evidence for this comes mainly from direct numerical simulations [5–7], but it is by no means clear what physics drives such a dynamo. One possibility that has received some attention is the shear-current effect [10], where an extra component of the mean electromotive force (EMF) is thought to result in the generation of the cross-shear component of the mean magnetic field from the component parallel to the shear flow. However, there is no agreement yet on whether the sign of such a coupling is favorable to the operation of a dynamo; some analytic calculations [11,12] and numerical experiments [5] find that the sign of the shear-current term is unfavorable for dynamo action.

A quasilinear kinematic theory of dynamo action in a linear shear flow of an incompressible fluid which has random velocity fluctuations was presented in [13], who used the "second order correlation approximation" (SOCA) in the limit of zero resistivity. Unlike earlier analytic work which treated shear as a small perturbation, this theory did not place any restriction on the strength of the shear. They arrived at an integrodifferential equation for the evolution of the mean magnetic field and argued that the shear-current-assisted dynamo is essentially absent. The theory was extended to take account of nonzero resistivity in [14]; this is again nonperturbative in the shear strength, uses SOCA, and is rigorously valid in the limit of small magnetic Reynolds number (Rm) but with no restriction on the fluid Reynolds number (Re). The kinematic approach to the *shear dynamo problem* taken in [13,14] uses in an essential manner the shearing coordinate transformation and the Galilean invariance (which is a fundamental symmetry of the problem) of the velocity fluctuations. The present work extends [14] by giving definite form to the statistics of the velocity field; specifically, the velocity field is assumed to obey the forced Navier-Stokes equation, in the absence of Lorentz forces.

In Sec. II we begin with a brief review of the salient results of [14]. The expression for the Galilean-invariant mean EMF is then worked out for the case of a mean magnetic field that is slowly varying in time. Thus the mean-field induction equation, which is an integrodifferential equation in the formulation of [14], now simplifies to a partial differential equation. This reduction is an essential first step to the later comparison with the numerical experiments of [5]. Explicit expressions for the transport coefficients α_{il} and η_{iml} are derived in terms of the two-point velocity correlators. We then recall some results from [14] which express the velocity correlators in terms of the velocity spectrum tensor. This tensorial quantity is real when the velocity field is nonhelical; we are able to prove that in this case, the transport coefficient α_{il} vanishes. Section III develops the dynamics of the velocity field at low Re, using the Navier-Stokes equation with stochastic external forcing. An explicit solution for the velocity field is presented and the velocity spectrum tensor is calculated in terms of the Galilean-invariant forcing statistics. For nonhelical forcing, the velocity field is also nonhelical and

*nishant@rri.res.in
†ssridhar@rri.res.in

the transport coefficient α_{il} vanishes, as noted above. We then specialize to the case when the forcing is not only nonhelical, but isotropic and delta correlated in time as well. In Sec. IV we specialize to the case when the mean field is a function only of the spatial coordinate X_3 and time τ; this reduction is necessary for comparison with the numerical experiments of [5]. Explicit expressions are derived for all four components of the magnetic diffusivity tensor $\eta_{ij}(\tau)$ in terms of the velocity power spectrum; the late-time saturation values η_{ij}^{∞} have direct bearing on the growth (or otherwise) of the mean magnetic field. Comparisons with earlier work—in particular [5]—are made, and the implications for the shear-current effect are discussed. We then conclude in Sec. V.

II. MEAN-FIELD ELECTRODYNAMICS IN A LINEAR SHEAR FLOW

A. Mean-field induction equation for small Rm

We begin with a brief review of the main results of [14]. Let $(\boldsymbol{e}_1,\boldsymbol{e}_2,\boldsymbol{e}_3)$ be the unit basis vectors of a Cartesian coordinate system in the laboratory frame. Using the notation $\boldsymbol{X}=(X_1,X_2,X_3)$ for the position vector and τ for time, we write the fluid velocity as $(SX_1\boldsymbol{e}_2+\boldsymbol{v})$, where S is the rate of shear parameter and $\boldsymbol{v}(\boldsymbol{X},\tau)$ is an incompressible and randomly fluctuating velocity field with zero mean. The mean magnetic field, $\boldsymbol{B}(\boldsymbol{X},\tau)$, obeys the following (mean-field induction) equation:

$$\left(\frac{\partial}{\partial\tau}+SX_1\frac{\partial}{\partial X_2}\right)\boldsymbol{B}-SB_1\boldsymbol{e}_2=\boldsymbol{\nabla}\times\boldsymbol{\mathcal{E}}+\eta\nabla^2\boldsymbol{B}, \quad (1)$$

where η is the microscopic resistivity and $\boldsymbol{\mathcal{E}}$ is the mean electromotive force (EMF), $\boldsymbol{\mathcal{E}}=\langle\boldsymbol{v}\times\boldsymbol{b}\rangle$, where $\boldsymbol{v}$ and $\boldsymbol{b}$ are the fluctuations in the velocity and magnetic fields.

To lowest order in Rm, the evolution of the magnetic field fluctuations, now denoted by $\boldsymbol{b}^{(0)}$, is governed by

$$\left(\frac{\partial}{\partial\tau}+SX_1\frac{\partial}{\partial X_2}\right)\boldsymbol{b}^{(0)}-Sb_1^{(0)}\boldsymbol{e}_2 =(\boldsymbol{B}\cdot\nabla)\boldsymbol{v}-(\boldsymbol{v}\cdot\nabla)\boldsymbol{B}+\eta\nabla^2\boldsymbol{b}^{(0)}. \quad (2)$$

This equation was solved by making a *shearing-coordinate transformation* to new space-time coordinates and new field variables. The new space-time variables $(\boldsymbol{x},t)$ are given by

$$x_1=X_1\,,\quad x_2=X_2-S\tau X_1\,,\quad x_3=X_3\,,\quad t=\tau\,, \quad (3)$$

where $\boldsymbol{x}$ may be thought of as the Lagrangian coordinates of a fluid element in the background shear flow. The new field variables are component-wise equal to the old variables:

$$\boldsymbol{H}(\boldsymbol{x},t)=\boldsymbol{B}(\boldsymbol{X},\tau),\quad \boldsymbol{h}(\boldsymbol{x},t)=\boldsymbol{b}^{(0)}(\boldsymbol{X},\tau),\quad \boldsymbol{u}(\boldsymbol{x},t)=\boldsymbol{v}(\boldsymbol{X},\tau). \quad (4)$$

In the new variables, Eq. (2) becomes

$$\frac{\partial\boldsymbol{h}}{\partial t}-Sh_1\boldsymbol{e}_2=\left(\boldsymbol{H}\cdot\frac{\partial}{\partial\boldsymbol{x}}-StH_1\frac{\partial}{\partial x_2}\right)\boldsymbol{u} -\left(\boldsymbol{u}\cdot\frac{\partial}{\partial\boldsymbol{x}}-Stu_1\frac{\partial}{\partial x_2}\right)\boldsymbol{H}+\eta\nabla^2\boldsymbol{h}. \quad (5)$$

We need the particular solution (i.e., the *forced solution*) which vanishes at $t=0$. This is given in component form as

$$\begin{aligned}h_m(\boldsymbol{x},t)=&\int_0^t dt'\int d^3x'\,G_\eta(\boldsymbol{x}-\boldsymbol{x}',t,t')\\&\times[u'_{ml}+S(t-t')\delta_{m2}u'_{1l}][H'_l-St'\delta_{l2}H'_1]\\&-\int_0^t dt'\int d^3x'\,G_\eta(\boldsymbol{x}-\boldsymbol{x}',t,t')\\&\times[H'_{ml}+S(t-t')\delta_{m2}H'_{1l}][u'_l-St'\delta_{l2}u'_1]. \quad (6)\end{aligned}$$

The primes in H'_l and u'_l mean that these functions are evaluated at $(\boldsymbol{x}',t')$. The quantities H'_{ml} and u'_{ml} are shorthand for $(\partial H'_m/\partial x'_l)$ and $(\partial u'_m/\partial x'_l)$, respectively. Here $G_\eta(\boldsymbol{r},t,t')$ is the *resistive Green's function* for the linear shear flow [14,15], which takes the form of a sheared heat kernel. The one property we will use is that $G_\eta(\boldsymbol{r},t,t')$ is an even function of $\boldsymbol{r}$. Otherwise, its spatial Fourier transform, defined by

$$\begin{aligned}\widetilde{G}_\eta(\boldsymbol{k},t,t')&=\int d^3r\,G_\eta(\boldsymbol{r},t,t')\exp[-\mathrm{i}\,\boldsymbol{k}\cdot\boldsymbol{r}]\\&=\exp\left[-\eta\left(k^2(t-t')-S\,k_1k_2(t^2-t'^2)+\frac{S^2}{3}k_2^2(t^3-t'^3)\right)\right], \quad (7)\end{aligned}$$

is more useful for our purposes.

The mean EMF is given by $\boldsymbol{\mathcal{E}}=\langle\boldsymbol{v}\times\boldsymbol{b}^{(0)}\rangle=\langle\boldsymbol{u}\times\boldsymbol{h}\rangle$, where Eq. (6) for $\boldsymbol{h}$ should be substituted. The averaging, $\langle\ \rangle$, acts only on the velocity variables but not the mean field; i.e., $\langle\boldsymbol{uuH}\rangle=\langle\boldsymbol{uu}\rangle\boldsymbol{H}$, etc. The $\boldsymbol{uu}$ velocity correlators can be rewritten in terms of the $\boldsymbol{vv}$ velocity correlators; this is a useful step because the latter are referred to the laboratory frame. The velocity correlators have a very important property called *Galilean invariance*, which is shared by *comoving observers*, who translate uniformly with the background shear flow. If a comoving observer is at position $\boldsymbol{\xi}=(\xi_1,\xi_2,\xi_3)$ at the initial time, then at a later time t, her location is given by

$$\boldsymbol{X}_c(\boldsymbol{\xi},t)=(\xi_1,\xi_2+St\,\xi_1,\xi_3). \quad (8)$$

Velocity fluctuations are defined to be Galilean invariant if and only if the statistical properties of the fluctuations, as seen by any comoving observer, are identical to the statistical properties seen in the laboratory frame; it follows that all comoving observers see the same statistics. There are two basic Galilean-invariant two-point velocity correlation functions, Q_{jml} and R_{jm}, which are defined as

$$Q_{jml}(\boldsymbol{r},t,t')=\left\langle v_j\left(\boldsymbol{X}_c\left(\frac{\boldsymbol{r}}{2},t\right),t\right)\frac{\partial v_m}{\partial X_l}\left(\boldsymbol{X}_c\left(-\frac{\boldsymbol{r}}{2},t'\right),t'\right)\right\rangle, \quad (9)$$

$$R_{jm}(\boldsymbol{r},t,t')=\left\langle v_j\left(\boldsymbol{X}_c\left(\frac{\boldsymbol{r}}{2},t\right),t\right)v_m\left(\boldsymbol{X}_c\left(-\frac{\boldsymbol{r}}{2},t'\right),t'\right)\right\rangle.$$

Then the mean EMF is a *functional* of the mean magnetic field, H_l, and its first spatial derivative, $H_{lm}=(\partial H_l/\partial x_m)$:

$$\begin{aligned}\mathcal{E}_i(\boldsymbol{x},t)=&\,\epsilon_{ijm}\int_0^t dt'\int d^3r\,G_\eta(\boldsymbol{r},t,t')\,C_{jml}(\boldsymbol{r},t,t')H_l(\boldsymbol{x}-\boldsymbol{r},t')\\&-\int_0^t dt'\int d^3r\,G_\eta(\boldsymbol{r},t,t')[\epsilon_{ijl}+S(t-t')\delta_{l1}\epsilon_{ij2}]\\&\times D_{jm}(\boldsymbol{r},t,t')H_{lm}(\boldsymbol{x}-\boldsymbol{r},t'), \quad (10)\end{aligned}$$

where C_{jml} and D_{jm} are two-point velocity correlators, which are derived from the more basic two-point velocity correlators

Q_{jml} and R_{jm} of Eqs. (9):

$$C_{jml}(\boldsymbol{r},t,t') = Q_{jml}(\boldsymbol{r},t,t') + S(t-t')\delta_{m2}\, Q_{j1l}(\boldsymbol{r},t,t'), \qquad (11)$$
$$D_{jm}(\boldsymbol{r},t,t') = R_{jm}(\boldsymbol{r},t,t') - St'\delta_{m2}\, R_{j1}(\boldsymbol{r},t,t').$$

Then the time evolution of the mean magnetic field is given in the new variables by

$$\frac{\partial \boldsymbol{H}}{\partial t} - SH_1\boldsymbol{e}_2 = \boldsymbol{\nabla}\times\boldsymbol{\mathcal{E}} + \eta\nabla^2\boldsymbol{H}, \qquad (12)$$
$$(\boldsymbol{\nabla})_p \equiv \frac{\partial}{\partial X_p} = \frac{\partial}{\partial x_p} - St\,\delta_{p1}\frac{\partial}{\partial x_2}.$$

Equations (12) and (10) form a closed system of integrodifferential equations, determining the time evolution of the mean magnetic field, $\boldsymbol{H}(\boldsymbol{x},t)$.

B. The mean EMF for a slowly varying magnetic field

The mean EMF given in Eq. (10) is a *functional* of H_l and H_{lm}. When the mean field is slowly varying compared to velocity correlation times, we expect to be able to approximate $\boldsymbol{\mathcal{E}}$ as a *function* of H_l and H_{lm}. In this case, the mean-field induction equation would reduce to a set of coupled partial differential equations, instead of the more formidable set of coupled integrodifferential equations given by (12) and (10). Sheared coordinates are essential for the calculations, but physical interpretation is simplest in the laboratory frame; hence we derive an expression for the mean EMF in terms of $\boldsymbol{B}(\boldsymbol{X},\tau)$.

The first step involves a Taylor expansion of the quantities H_l and H_{lm} occurring in Eq. (10) for the mean EMF. Neglecting space-time derivatives higher than the first-order ones, we have

$$H_l(\boldsymbol{x}-\boldsymbol{r},t') = H_l(\boldsymbol{x},t) - r_pH_{lp}(\boldsymbol{x},t) - (t-t')\frac{\partial H_l(\boldsymbol{x},t)}{\partial t} + \cdots,$$
$$H_{lm}(\boldsymbol{x}-\boldsymbol{r},t') = H_{lm}(\boldsymbol{x},t) - (t-t')\frac{\partial H_{lm}(\boldsymbol{x},t)}{\partial t} + \cdots. \qquad (13)$$

We now use the mean-field induction equation (12) to express $(\partial\boldsymbol{H}/\partial t)$ in terms of spatial derivatives. Let L be the spatial scale over which the mean field varies. When the mean field varies slowly, L is large and the contributions from both the resistive term and the mean EMF are small, as is shown below. Let ℓ and $v_{\rm rms}$ be the spatial scale and root-mean-squared amplitude of the velocity fluctuations. The resistive term makes a contribution of order $(\ell/L)^2{\rm Rm}^{-1}$, which we now assume is much less than unity. Using Eq. (10), we can verify that $\boldsymbol{\nabla}\times\boldsymbol{\mathcal{E}}$ contributes terms of five different orders: (ℓ/L), $(\ell/L)(S\ell/v_{\rm rms})$, $(\ell/L)^2$, $(\ell/L)^2(S\ell/v_{\rm rms})$, and $(\ell/L)^2(S\ell/v_{\rm rms})^2$. These are all small when (ℓ/L) and $(\ell/L)(S\ell/v_{\rm rms})$ are both much smaller than unity. That we must have $(\ell/L)\ll 1$ is natural from the familiar case of zero shear. The presence of shear introduces an additional requirement that $(\ell/L)(S\ell/v_{\rm rms})\ll 1$. We now define the small parameter, $\mu \ll 1$, to be equal to the largest of the three small quantities, $(\ell/L)^2{\rm Rm}^{-1}\ll 1$, $(\ell/L)\ll 1$, and $(\ell/L)(S\ell/v_{\rm rms})\ll 1$. Then,

$$\frac{\partial H_l}{\partial t} = S\delta_{l2}H_1 + O(\mu), \qquad (14)$$

and Eqs. (13) give

$$H_l(\boldsymbol{x}-\boldsymbol{r},t') = H_l(\boldsymbol{x},t) - r_pH_{lp}(\boldsymbol{x},t) - S(t-t')\delta_{l2}H_1 + O(\mu), \qquad (15)$$
$$H_{lm}(\boldsymbol{x}-\boldsymbol{r},t') = H_{lm}(\boldsymbol{x},t) - S(t-t')\delta_{l2}H_{1m} + O(\mu).$$

We substitute Eq. (15) in (10) to get

$$\mathcal{E}_i(\boldsymbol{x},t) = \epsilon_{ijm}\,H_l(\boldsymbol{x},t)\int_0^t dt'\int d^3r\,G_\eta(\boldsymbol{r},t,t')\,[C_{jml}(\boldsymbol{r},t,t') - S(t-t')\,\delta_{l1}\,C_{jm2}(\boldsymbol{r},t,t')]$$
$$-\,\epsilon_{ijm}\,H_{lp}(\boldsymbol{x},t)\int_0^t dt'\int d^3r\;r_p\,G_\eta(\boldsymbol{r},t,t')\,C_{jml}(\boldsymbol{r},t,t') - \epsilon_{ijl}\,H_{lm}(\boldsymbol{x},t)\int_0^t dt'\int d^3r\,G_\eta(\boldsymbol{r},t,t')\,D_{jm}(\boldsymbol{r},t,t') + O(\mu^2). \qquad (16)$$

The final step is to rewrite the above expression in terms of the original magnetic field variable, using

$$H_l(\boldsymbol{x},t) = B_l(\boldsymbol{X},\tau),$$
$$H_{lm}(\boldsymbol{x},t) \equiv \frac{\partial H_l(\boldsymbol{x},t)}{\partial x_m} = \left(\frac{\partial}{\partial X_m} + S\tau\delta_{m1}\frac{\partial}{\partial X_2}\right)B_l(\boldsymbol{X},\tau). \qquad (17)$$

Therefore, for a slowly varying magnetic field, the mean EMF is given by

$$\mathcal{E}_i = \alpha_{il}(\tau)B_l(\boldsymbol{X},\tau) - \eta_{iml}(\tau)\frac{\partial B_l(\boldsymbol{X},\tau)}{\partial X_m}, \qquad (18)$$

where the *transport coefficients* are given by

$$\alpha_{il}(\tau) = \epsilon_{ijm}\int_0^\tau d\tau'\int d^3r\,G_\eta(\boldsymbol{r},\tau,\tau')\,[C_{jml}(\boldsymbol{r},\tau,\tau') - S(\tau-\tau')\,\delta_{l1}\,C_{jm2}(\boldsymbol{r},\tau,\tau')],$$
$$\eta_{iml}(\tau) = \epsilon_{ijp}\int_0^\tau d\tau'\int d^3r\,[r_m + S\tau\delta_{m2}r_1]\,G_\eta(\boldsymbol{r},\tau,\tau')\,C_{jpl}(\boldsymbol{r},\tau,\tau')$$
$$+\,\epsilon_{ijl}\int_0^\tau d\tau'\int d^3r\,G_\eta(\boldsymbol{r},\tau,\tau')\,[D_{jm}(\boldsymbol{r},\tau,\tau') + S\tau\delta_{m2}D_{j1}(\boldsymbol{r},\tau,\tau')]. \qquad (19)$$

Then the mean-field induction equation (1), together with Eqs. (18) and (19), is a closed partial differential equation (which is first order in temporal and second order in spatial derivatives).

C. Velocity correlators expressed in terms of the velocity spectrum tensor

The Galilean invariance of the two-point velocity correlators can be stated most compactly in Fourier space. Let $\tilde{\boldsymbol{v}}(\boldsymbol{K},\tau)$ be the spatial Fourier transform of $\boldsymbol{v}(\boldsymbol{X},\tau)$, defined by

$$\tilde{\boldsymbol{v}}(\boldsymbol{K},\tau) = \int d^3X\, \boldsymbol{v}(\boldsymbol{X},\tau)\, \exp[-\mathrm{i}\boldsymbol{K}\cdot\boldsymbol{X}], \qquad [\boldsymbol{K}\cdot\tilde{\boldsymbol{v}}(\boldsymbol{K},\tau)] = 0. \tag{20}$$

New Fourier variables are defined by the Fourier-space *shearing transformation*,

$$k_1 = K_1 + S\tau K_2, \quad k_2 = K_2, \quad k_3 = K_3, \quad t = \tau. \tag{21}$$

It is proved in [14] that a Galilean-invariant Fourier-space two-point velocity correlator must be of the form

$$\langle \tilde{v}_j(\boldsymbol{K},\tau)\, \tilde{v}_m^*(\boldsymbol{K}',\tau')\rangle = (2\pi)^6\, \delta(\boldsymbol{k}-\boldsymbol{k}')\, \Pi_{jm}(\boldsymbol{k},t,t'), \tag{22}$$

where Π_{jm} is the *velocity spectrum tensor*, which must possess the following properties:

$$\begin{gathered}\Pi_{ij}(\boldsymbol{k},t,t') = \Pi_{ij}^*(-\boldsymbol{k},t,t') = \Pi_{ji}(-\boldsymbol{k},t',t),\\ K_i\, \Pi_{ij}(\boldsymbol{k},t,t') = (k_i - St\,\delta_{i1}k_2)\,\Pi_{ij}(\boldsymbol{k},t,t') = 0,\\ K_j'\, \Pi_{ij}(\boldsymbol{k},t,t') = (k_j - St'\,\delta_{j1}k_2)\Pi_{ij}(\boldsymbol{k},t,t') = 0.\end{gathered} \tag{23}$$

Now, the various two-point velocity correlators can be written as

$$\begin{aligned}
R_{jm}(\boldsymbol{r},t,t') &= \int d^3k\, \Pi_{jm}(\boldsymbol{k},t,t')\, \exp[\mathrm{i}\,\boldsymbol{k}\cdot\boldsymbol{r}],\\
Q_{jml}(\boldsymbol{r},t,t') &= -\mathrm{i}\int d^3k\, [k_l - St'\delta_{l1}k_2]\, \Pi_{jm}(\boldsymbol{k},t,t')\, \exp[\mathrm{i}\,\boldsymbol{k}\cdot\boldsymbol{r}],\\
D_{jm}(\boldsymbol{r},t,t') &= \int d^3k\, [\Pi_{jm}(\boldsymbol{k},t,t') - St'\delta_{m2}\,\Pi_{j1}(\boldsymbol{k},t,t')]\exp[\mathrm{i}\,\boldsymbol{k}\cdot\boldsymbol{r}],\\
C_{jml}(\boldsymbol{r},t,t') &= -\mathrm{i}\int d^3k[k_l - St'\delta_{l1}k_2][\Pi_{jm}(\boldsymbol{k},t,t') + S(t-t')\delta_{m2}\Pi_{j1}(\boldsymbol{k},t,t')]\exp[\mathrm{i}\,\boldsymbol{k}\cdot\boldsymbol{r}].
\end{aligned} \tag{24}$$

Using the above expressions for D_{jm} and C_{jml} in Eqs. (19), the transport coefficients $\alpha_{il}(\tau)$ and $\eta_{iml}(\tau)$ can also be written in terms of the velocity spectrum tensor.

The *correlation helicity* may be defined as

$$H_{\mathrm{cor}}(t,t') = \epsilon_{jlm}\langle v_j(\boldsymbol{0},t)\, v_{ml}(\boldsymbol{0},t')\rangle = \mathrm{i}\int d^3k\, [k_l - St'\delta_{l1}k_2]\epsilon_{ljm}\Pi_{jm}(\boldsymbol{k},t,t'). \tag{25}$$

From the first of Eqs. (23), it is clear that the real part of $\Pi_{jm}(\boldsymbol{k},t,t')$ is an even function of $\boldsymbol{k}$, whereas the imaginary part is an odd function of $\boldsymbol{k}$. Hence only the imaginary part of $\Pi_{jm}(\boldsymbol{k},t,t')$ contributes to the correlation helicity. We shall see that the forced velocity fields we deal with later in this article possess a real velocity spectrum, and their correlation helicity vanishes. In this case,

$$\begin{aligned}
Q_{jml}(\boldsymbol{r},t,t') &= \int d^3k\, [k_l - St'\delta_{l1}k_2]\, \Pi_{jm}(\boldsymbol{k},t,t')\, \sin[\boldsymbol{k}\cdot\boldsymbol{r}],\\
C_{jml}(\boldsymbol{r},t,t') &= \int d^3k[k_l - St'\delta_{l1}k_2][\Pi_{jm}(\boldsymbol{k},t,t') + S(t-t')\delta_{m2}\Pi_{j1}(\boldsymbol{k},t,t')]\sin[\boldsymbol{k}\cdot\boldsymbol{r}]
\end{aligned} \tag{26}$$

are both *odd* functions of $\boldsymbol{r}$. Since the resistive Green's function, $G_\eta(\boldsymbol{r},t,t')$, is an *even* function of $\boldsymbol{r}$, Eq. (19) implies that the *transport coefficient* $\alpha_{il}(\tau)$ *vanishes*.

III. FORCED STOCHASTIC VELOCITY DYNAMICS

A. Forced velocity dynamics for small Re

We consider the simplest of dynamics for the velocity field by ignoring Lorentz forces, and assuming that the fluid is stirred randomly by some external means. If the velocity fluctuations have root-mean-squared (rms) amplitude v_{rms} on some typical spatial scale ℓ, the fluid Reynolds number may be defined as $\mathrm{Re} = (v_{\mathrm{rms}}\ell/\nu)$, where ν is the kinematic viscosity; note that Re has been defined with respect to the fluctuation velocity field, not the background shear velocity field. In the limit of small Reynolds number ($\mathrm{Re} \ll 1$), the nonlinear term in the Navier-Stokes equation may be ignored. Then the dynamics of the velocity field, $\boldsymbol{v}(\boldsymbol{X},\tau)$, is governed by the randomly forced, linearized Navier-Stokes equation,

$$\left(\frac{\partial}{\partial\tau} + SX_1\frac{\partial}{\partial X_2}\right)\boldsymbol{v} + Sv_1\boldsymbol{e}_2 = -\nabla p + \nu\nabla^2\boldsymbol{v} + \boldsymbol{f}. \tag{27}$$

$\boldsymbol{f}(\boldsymbol{X},\tau)$ is the random stirring force per unit mass which is assumed to be divergence-free with zero mean: $\nabla\cdot\boldsymbol{f} = 0$ and $\langle\boldsymbol{f}\rangle = \boldsymbol{0}$. The pressure variable p is determined by requiring that Eq. (27) preserve the condition $\nabla\cdot\boldsymbol{v} = 0$. Then p satisfies the Poisson equation,

$$\nabla^2 p = -2S\frac{\partial v_1}{\partial X_2}. \tag{28}$$

It should be noted that the linearity of Eqs. (27) and (28) implies that the velocity fluctuations have zero mean, $\langle\boldsymbol{v}\rangle = \boldsymbol{0}$. It is clear from Eq. (28) that p is a nonlocal function of the velocity field, so it is best to work in Fourier space. Taking the spatial Fourier transform of Eq. (27), we can see that the Fourier transform of the velocity field, $\tilde{\boldsymbol{v}}(\boldsymbol{K},\tau)$, obeys

$$\left(\frac{\partial}{\partial\tau} - SK_2\frac{\partial}{\partial K_1} + \nu K^2\right)\tilde{v}_i - 2S\left(\frac{K_2K_i}{K^2} - \frac{\delta_{i2}}{2}\right)\tilde{v}_1 = \tilde{f}_i, \tag{29}$$

where $\tilde{f}_i(\boldsymbol{K},\tau)$ is the spatial Fourier transform of f_i. It can be verified that Eq. (29) preserves the incompressibility condition $K_m\tilde{v}_m = 0$.

We can get rid of the inhomogeneous term, $(K_2\partial/\partial K_1)$, in Eq. (29) by transforming from the old variables $(\boldsymbol{K},\tau)$ to new variables $(\boldsymbol{k},t)$, through the Fourier-space shearing transformation of Eq. (21). First, we need to define new velocity and forcing variables, $a_i(\boldsymbol{k},t)$ and $g_i(\boldsymbol{k},t)$, respectively, by

$$\tilde{v}_i(\boldsymbol{K},\tau) = \widetilde{G}_\nu(\boldsymbol{k},t,0)\, a_i(\boldsymbol{k},t), \tag{30}$$

$$\tilde{f}_i(\boldsymbol{K},\tau) = \widetilde{G}_\nu(\boldsymbol{k},t,0)\, g_i(\boldsymbol{k},t), \tag{31}$$

where $\widetilde{G}_\nu(\boldsymbol{k},t,0)$ is the Fourier-space *viscous Green's function*, defined by

$$\widetilde{G}_\nu(\boldsymbol{k},t,t') = \exp\left[-\nu\int_{t'}^{t} ds\, K^2(\boldsymbol{k},s)\right]. \tag{32}$$

Noting the fact that $\boldsymbol{K}(\boldsymbol{k},s) = (k_1 - Ssk_2,k_2,k_3)$ and $K^2(\boldsymbol{k},s) = |\boldsymbol{K}(\boldsymbol{k},s)|^2$, the viscous Green's function can be calculated in explicit form as

$$\widetilde{G}_\nu(\boldsymbol{k},t,t') = \exp\left[-\nu\left(k^2(t-t') - S\,k_1\,k_2\,(t^2-t'^2) + \frac{S^2}{3}k_2^2(t^3-t'^3)\right)\right]. \tag{33}$$

The Green's function possesses the following properties:

$$\begin{aligned}\widetilde{G}_\nu(\boldsymbol{k},t,t') &= \widetilde{G}_\nu(-\boldsymbol{k},t,t'),\\ \widetilde{G}_\nu(k_1,k_2,k_3,t,t') &= \widetilde{G}_\nu(k_1,k_2,-k_3,t,t'),\\ \widetilde{G}_\nu(\boldsymbol{k},t,t') = \widetilde{G}_\nu(\boldsymbol{k},t,s)&\times\widetilde{G}_\nu(\boldsymbol{k},s,t'),\quad \text{for any s.}\end{aligned} \tag{34}$$

Using the inverse transformation,

$$K_1 = k_1 - Stk_2,\quad K_2 = k_2,\quad K_3 = k_3,\quad \tau = t, \tag{35}$$

and the fact that partial derivatives transform as

$$\frac{\partial}{\partial K_j} = \frac{\partial}{\partial k_j} + St\delta_{j2}\frac{\partial}{\partial k_1},\quad \frac{\partial}{\partial \tau} = \frac{\partial}{\partial t} + Sk_2\frac{\partial}{\partial k_1}, \tag{36}$$

Eq. (29) leads to the following equation for the new velocity variables, $a_i(\boldsymbol{k},t)$:

$$\frac{\partial a_i}{\partial t} - 2S\left(\frac{K_2K_i}{K^2} - \frac{\delta_{i2}}{2}\right)a_1 = g_i\,, \tag{37}$$

where $\boldsymbol{K}(\boldsymbol{k},t) = (k_1 - Stk_2,k_2,k_3)$ and $K^2(\boldsymbol{k},t) = |\boldsymbol{K}(\boldsymbol{k},t)|^2$ as given by Eq. (35). It can be verified that Eq. (37) preserves the dot product, $K_ia_i = 0$. We also note that the dependence of the velocities $\tilde{v}_i(\boldsymbol{K},\tau)$ on the viscosity ν arises solely through the Fourier-space Green's function. It is helpful to display in explicit form all three components of Eq. (37):

$$\frac{\partial a_1}{\partial t} - 2S\left(\frac{K_1K_2}{K^2}\right)a_1 = g_1\,, \tag{38}$$

$$\frac{\partial a_2}{\partial t} - 2S\left(\frac{K_2^2}{K^2} - \frac{1}{2}\right)a_1 = g_2\,, \tag{39}$$

$$\frac{\partial a_3}{\partial t} - 2S\left(\frac{K_2K_3}{K^2}\right)a_1 = g_3\,. \tag{40}$$

Then Eq. (38) can be solved to get an explicit expression for $a_1(\boldsymbol{k},t)$. When this is substituted in Eqs. (39) and (40), they can be integrated directly to obtain expressions for $a_2(\boldsymbol{k},t)$ and $a_3(\boldsymbol{k},t)$. The *forced* (or particular) solution, with initial condition $a_i(\boldsymbol{k},0) = 0$, is

$$a_i(\boldsymbol{k},t) = \int_0^t ds\, g_i(\boldsymbol{k},s) + \int_0^t ds\,[\Lambda_i(\boldsymbol{K}(\boldsymbol{k},t)) - \Lambda_i(\boldsymbol{K}(\boldsymbol{k},s))]\,\frac{K^2(\boldsymbol{k},s)}{K_\perp^2}\,g_1(\boldsymbol{k},s)\,, \tag{41}$$

where $K_\perp^2 \equiv K_2^2 + K_3^2 = k_2^2 + k_3^2 \equiv k_\perp^2$, and the function Λ_i is defined as

$$\Lambda_i(\boldsymbol{K}) = \delta_{i1} - \frac{K_1K_i}{K^2} + \frac{K_3}{K_\perp}\left[\frac{K_3}{K_2}\delta_{i2} - \delta_{i3}\right]\arctan\left(\frac{K_1}{K_\perp}\right). \tag{42}$$

B. Velocity spectrum tensor expressed in terms of the forcing

Our goal is to express the velocity spectrum tensor in terms of the statistical properties of the forcing. If the forcing is Galilean invariant, then we must have

$$\langle \tilde{f}_j(\boldsymbol{K},\tau)\,\tilde{f}_m^*(\boldsymbol{K}',\tau')\rangle = (2\pi)^6\,\delta(\boldsymbol{k}-\boldsymbol{k}')\Phi_{jm}(\boldsymbol{k},t,t'), \tag{43}$$

where Φ_{jm} is the *forcing spectrum tensor*. We are now ready to use the dynamical solution of the last subsection. Using Eqs. (30) and (41), the Fourier-space, unequal-time, two-point velocity correlator is given by

$$\begin{aligned}\langle \tilde{v}_j(\boldsymbol{K},\tau)\,\tilde{v}_m^*(\boldsymbol{K}',\tau')\rangle \;=\; &\widetilde{G}_\nu(\boldsymbol{k},t,0)\,\widetilde{G}_\nu(\boldsymbol{k}',t',0)\langle\tilde{a}_j(\boldsymbol{k},t)\,\tilde{a}_m^*(\boldsymbol{k}',t')\rangle = \widetilde{G}_\nu(\boldsymbol{k},t,0)\,\widetilde{G}_\nu(\boldsymbol{k}',t',0)\int_0^t ds\int_0^{t'} ds'\\ &\times\Bigg\{\langle g_j(\boldsymbol{k},s)\,g_m^*(\boldsymbol{k}',s')\rangle + [\Lambda_j(\boldsymbol{K}(\boldsymbol{k},t)) - \Lambda_j(\boldsymbol{K}(\boldsymbol{k},s))]\frac{K^2(\boldsymbol{k},s)}{K_\perp^2}\langle g_1(\boldsymbol{k},s)\,g_m^*(\boldsymbol{k}',s')\rangle\\ &+[\Lambda_m(\boldsymbol{K}(\boldsymbol{k}',t')) - \Lambda_m(\boldsymbol{K}(\boldsymbol{k}',s'))]\frac{K^2(\boldsymbol{k}',s')}{K_\perp'^2}\langle g_j(\boldsymbol{k},s)\,g_1^*(\boldsymbol{k}',s')\rangle + [\Lambda_j(\boldsymbol{K}(\boldsymbol{k},t)) - \Lambda_j(\boldsymbol{K}(\boldsymbol{k},s))]\\ &\times[\Lambda_m(\boldsymbol{K}(\boldsymbol{k}',t')) - \Lambda_m(\boldsymbol{K}(\boldsymbol{k}',s'))]\frac{K^2(\boldsymbol{k},s)K^2(\boldsymbol{k}',s')}{K_\perp^2K_\perp'^2}\langle g_1(\boldsymbol{k},s)\,g_1^*(\boldsymbol{k}',s')\rangle\Bigg\}.\end{aligned} \tag{44}$$

Using Eqs. (31) and (43), we write

$$\begin{aligned}\langle g_j(\boldsymbol{k},s)\,g_m^*(\boldsymbol{k}',s')\rangle &= \frac{1}{\widetilde{G}_\nu(\boldsymbol{k},s,0)\,\widetilde{G}_\nu(\boldsymbol{k}',s',0)}\langle\tilde{f}_j(\boldsymbol{K}(\boldsymbol{k},s),s)\,\tilde{f}_m^*(\boldsymbol{K}(\boldsymbol{k}',s'),s')\rangle\\ &= \frac{1}{\widetilde{G}_\nu(\boldsymbol{k},s,0)\,\widetilde{G}_\nu(\boldsymbol{k}',s',0)}(2\pi)^6\,\delta(\boldsymbol{k}-\boldsymbol{k}')\Phi_{jm}(\boldsymbol{k},s,s').\end{aligned} \tag{45}$$

Using $\widetilde{G}_\nu(\boldsymbol{k},t,0)[\widetilde{G}_\nu(\boldsymbol{k},s,0)]^{-1} = \widetilde{G}_\nu(\boldsymbol{k},t,s)$, Eqs. (44), (45), and (22) give

$$\begin{aligned}\Pi_{jm}(\boldsymbol{k},t,t') = \int_0^t ds \int_0^{t'} ds'\, \widetilde{G}_\nu(\boldsymbol{k},t,s)\,\widetilde{G}_\nu(\boldsymbol{k},t',s')\Big\{\Phi_{jm}(\boldsymbol{k},s,s') + [\Lambda_j(\boldsymbol{K}(\boldsymbol{k},t)) - \Lambda_j(\boldsymbol{K}(\boldsymbol{k},s))]\frac{K^2(\boldsymbol{k},s)}{K_\perp^2}\Phi_{1m}(\boldsymbol{k},s,s')\\ + [\Lambda_m(\boldsymbol{K}(\boldsymbol{k},t')) - \Lambda_m(\boldsymbol{K}(\boldsymbol{k},s'))]\frac{K^2(\boldsymbol{k},s')}{K_\perp^2}\Phi_{j1}(\boldsymbol{k},s,s') + [\Lambda_j(\boldsymbol{K}(\boldsymbol{k},t)) - \Lambda_j(\boldsymbol{K}(\boldsymbol{k},s))]\\ \times [\Lambda_m(\boldsymbol{K}(\boldsymbol{k},t')) - \Lambda_m(\boldsymbol{K}(\boldsymbol{k},s'))]\frac{K^2(\boldsymbol{k},s)K^2(\boldsymbol{k},s')}{K_\perp^4}\,\Phi_{11}(\boldsymbol{k},s,s')\Big\}.\end{aligned} \tag{46}$$

When $\Phi_{jm}(\boldsymbol{k},t,t')$ is real, the forcing may be called nonhelical. Then Eq. (46) proves that the velocity spectrum tensor $\Pi_{jm}(\boldsymbol{k},t,t')$ is also a real quantity. In other words, nonhelical forcing of an incompressible fluid at low Re, in the absence of Lorentz forces, gives rise to a nonhelical velocity field. In this case, as we noted earlier, the velocity correlators $Q_{jml}(\boldsymbol{r},t,t')$ and $C_{jml}(\boldsymbol{r},t,t')$ are odd functions of $\boldsymbol{r}$ and, $G_\eta(\boldsymbol{r},t,t')$ being an even function of $\boldsymbol{r}$, Eq. (19) implies that the transport coefficient $\alpha_{il}(\tau)$ vanishes. In other words, the α effect is absent for nonhelical forcing at low Re and Rm, for arbitrary values of the shear parameter. This may not seem like a particularly surprising conclusion, but it is by no means an obvious one, because at high Re it may happen that $\Pi_{jm}(\boldsymbol{k},t,t')$ is complex even when $\Phi_{jm}(\boldsymbol{k},t,t')$ is real.

We now specialize to the case when the forcing is not only *nonhelical*, but *isotropic* and *delta correlated in time* as well; in this case,

$$\Phi_{jm}(\boldsymbol{k},s,s') = \delta(s-s')\,P_{jm}(\boldsymbol{K}(\boldsymbol{k},s))\,F\left(\frac{K(\boldsymbol{k},s)}{K_F}\right), \tag{47}$$

where $K(\boldsymbol{k},s) = |\boldsymbol{K}(\boldsymbol{k},s)|$, $K_F = \ell^{-1}$ is the wave number at which the fluid is stirred, $P_{jm}(\boldsymbol{K}) = (\delta_{jm} - K_jK_m/K^2)$ is a projection operator, and $F(K/K_F) \geqslant 0$ is the *forcing power spectrum*.

Substitute Eq. (47) in (46), and reduce the double-time integrals to a single-time integral using

$$\int_0^t ds \int_0^{t'} ds'\,\delta(s-s')\,w(\boldsymbol{k},s,s') = \int_0^{t_<} ds\, w(\boldsymbol{k},s,s), \tag{48}$$

where $t_< = \min(t,t')$. Then the velocity spectrum tensor,

$$\begin{aligned}\Pi_{jm}(\boldsymbol{k},t,t') = \int_0^{t_<} ds\,\widetilde{G}_\nu(\boldsymbol{k},t,s)\,\widetilde{G}_\nu(\boldsymbol{k},t',s)\,F\left(\frac{K(\boldsymbol{k},s)}{K_F}\right)\Big\{P_{jm}(\boldsymbol{K}(\boldsymbol{k},s)) + [\Lambda_j(\boldsymbol{K}(\boldsymbol{k},t)) - \Lambda_j(\boldsymbol{K}(\boldsymbol{k},s))]\frac{K^2(\boldsymbol{k},s)}{K_\perp^2}P_{1m}(\boldsymbol{K}(\boldsymbol{k},s))\\ + [\Lambda_m(\boldsymbol{K}(\boldsymbol{k},t')) - \Lambda_m(\boldsymbol{K}(\boldsymbol{k},s))]\frac{K^2(\boldsymbol{k},s)}{K_\perp^2}P_{j1}(\boldsymbol{K}(\boldsymbol{k},s)) + [\Lambda_j(\boldsymbol{K}(\boldsymbol{k},t)) - \Lambda_j(\boldsymbol{K}(\boldsymbol{k},s))]\\ \times [\Lambda_m(\boldsymbol{K}(\boldsymbol{k},t')) - \Lambda_m(\boldsymbol{K}(\boldsymbol{k},s))]\frac{K^4(\boldsymbol{k},s)}{K_\perp^4}\,P_{11}(\boldsymbol{K}(\boldsymbol{k},s))\Big\},\end{aligned} \tag{49}$$

is completely determined when the forcing power spectrum, $F(K/K_F)$, has been specified.

Let an observer located at the origin of the laboratory frame correlate fluid velocities at time $\tau = t$ and at time $\tau' = t'$. The two-point function that measures this quantity is given by

$$\langle v_j(\boldsymbol{0},\tau)v_m(\boldsymbol{0},\tau')\rangle = R_{jm}(\boldsymbol{0},t,t') = \int d^3k\;\Pi_{jm}(\boldsymbol{k},t,t'). \tag{50}$$

It can be proved that, in the long time limit when $t \to \infty$ and $t' \to \infty$, $R_{jm}(\boldsymbol{0},t,t')$ is a function only of the time difference, $(t-t')$. The *equal-time* correlator, defined by $R_{jm}(\boldsymbol{0},t,t)$, is symmetric: $R_{jm}(\boldsymbol{0},t,t) = R_{mj}(\boldsymbol{0},t,t)$. A related quantity is the root-mean-squared velocity, $v_{\rm rms}(t)$, defined by

$$v_{\rm rms}^2(t) = R_{11}(\boldsymbol{0},t,t) + R_{22}(\boldsymbol{0},t,t) + R_{33}(\boldsymbol{0},t,t). \tag{51}$$

In the long-time limit, both $R_{jm}(\boldsymbol{0},t,t)$ and $v_{\rm rms}(t)$ saturate due to the balance reached between forcing and viscous dissipation; let $v_{\rm rms}^\infty = \lim_{t\to\infty} v_{\rm rms}(t)$.

We now define various dimensionless quantities: the *fluid Reynolds number*, $\mathrm{Re} = v_{\rm rms}^\infty/(\nu K_F)$; the *magnetic Reynolds number*, $\mathrm{Rm} = v_{\rm rms}^\infty/(\eta K_F)$; the *Prandtl number*, $\mathrm{Pr} = \nu/\eta$; and the dimensionless *Shear parameter*, $S_h = S/(v_{\rm rms}^\infty K_F)$.

For numerical computations, it is necessary to choose a form for the forcing power spectrum. A quite common choice, used especially in numerical simulations, is forcing which is confined to a spherical shell of magnitude K_F. Therefore, whenever we need to choose a form for the forcing power spectrum, we take it to be

$$F\left(\frac{K}{K_F}\right) = F_0\,\delta\left(\frac{K}{K_F} - 1\right). \tag{52}$$

IV. PREDICTIONS AND COMPARISON WITH NUMERICAL EXPERIMENTS

We have already established that the transport coefficient $\alpha_{il} = 0$ when the stirring is nonhelical. The other transport coefficient η_{iml} can be calculated by the following steps:

(1) Computing the velocity spectrum tensor Π_{jm} using Eqs. (49) and (52).

(2) Using this in Eq. (24) to compute the velocity correlators C_{jml} and D_{jm}.

(3) Substituting these correlators in the second of Eqs. (19).

We also seek to compare our analytical results with measurements of numerical simulations, which use the test-field method [5]. In this method, the mean magnetic field is averaged over the coordinates X_1 and X_2. So we consider the case when the mean magnetic field $\boldsymbol{B} = \boldsymbol{B}(X_3,\tau)$. The condition $\nabla\cdot\boldsymbol{B} = 0$ implies that B_3 is uniform in space, and it can be set to zero; hence we have $\boldsymbol{B} = (B_1, B_2, 0)$. Thus, Eq. (18) for the mean EMF gives $\boldsymbol{\mathcal{E}} = (\mathcal{E}_1, \mathcal{E}_2, 0)$, with

$$\mathcal{E}_i = -\eta_{ij}(\tau)\,J_j, \quad \boldsymbol{J} = \nabla\times\boldsymbol{B} = \left(-\frac{\partial B_2}{\partial X_3}, \frac{\partial B_1}{\partial X_3}, 0\right), \tag{53}$$

where 2-indexed magnetic diffusivity tensor η_{ij} has four components $(\eta_{11}, \eta_{12}, \eta_{21}, \eta_{22})$, which are defined in terms of the 3-indexed object η_{iml} by

$$\eta_{ij}(\tau) = \epsilon_{lj3}\,\eta_{i3l}(\tau), \text{ which implies that } \eta_{i1}(\tau) = -\eta_{i32}(\tau), \quad \eta_{i2}(\tau) = \eta_{i31}(\tau). \tag{54}$$

Equation (53) for $\boldsymbol{\mathcal{E}}$ can now be substituted in Eq. (1). Then the mean-field induction becomes

$$\begin{aligned} \frac{\partial B_1}{\partial \tau} &= -\eta_{21}\,\frac{\partial^2 B_2}{\partial X_3^2} + (\eta + \eta_{22})\frac{\partial^2 B_1}{\partial X_3^2}, \\ \frac{\partial B_2}{\partial \tau} &= SB_1 - \eta_{12}\,\frac{\partial^2 B_1}{\partial X_3^2} + (\eta + \eta_{11})\frac{\partial^2 B_2}{\partial X_3^2}. \end{aligned} \tag{55}$$

The diagonal components, $\eta_{11}(\tau)$ and $\eta_{22}(\tau)$, augment the microscopic resistivity, η, whereas the off-diagonal components, $\eta_{12}(\tau)$ and $\eta_{21}(\tau)$, lead to cross-coupling of B_1 and B_2.

A. The magnetic diffusivity tensor

We now use our dynamical theory to calculate $\eta_{ij}(\tau)$. From Eqs. (54) and (19), we have

$$\begin{aligned} \eta_{ij}(\tau) &= \epsilon_{lj3}\,\eta_{i3l}(\tau) \\ &= \epsilon_{lj3}\epsilon_{ipm}\int_0^\tau d\tau' \int d^3r\, r_3\, G_\eta(\boldsymbol{r},\tau,\tau')\, C_{pml}(\boldsymbol{r},\tau,\tau') \\ &\quad + \delta_{ij}\int_0^\tau d\tau' \int d^3r\, G_\eta(\boldsymbol{r},\tau,\tau')\, D_{33}(\boldsymbol{r},\tau,\tau'). \end{aligned} \tag{56}$$

Thus the D terms contribute only to the diagonal components, η_{11} and η_{22}. This is the expected behavior of turbulent diffusion, which we now see is true for arbitrary shear. Using Eq. (24), the velocity correlators C_{pml} and D_{33} can now be written in terms of Π_{jm}. After some lengthy calculations, the $\eta_{ij}(\tau)$ can be expressed in terms of the velocity spectrum tensor by

$$\begin{aligned} \eta_{ij}(\tau) = 2\eta \int_0^\tau d\tau' \int d^3k\, \widetilde{G}_\eta(\boldsymbol{k},\tau,\tau')(\tau-\tau')k_3\,[\delta_{j2}(k_1 - S\tau' k_2) - \delta_{j1}k_2] \\ \times [\delta_{i1}(\Pi_{23} - \Pi_{32} - S(\tau-\tau')\Pi_{31}) + \delta_{i2}(\Pi_{31} - \Pi_{13})] + \delta_{ij}\int_0^\tau d\tau' \int d^3k\, \widetilde{G}_\eta(\boldsymbol{k},\tau,\tau')\,\Pi_{33}\,, \end{aligned} \tag{57}$$

where $\Pi_{lm} = \Pi_{lm}(\boldsymbol{k},\tau,\tau')$, and the indices (i,j) run over values 1 and 2. Here $\widetilde{G}_\eta(\boldsymbol{k},\tau,\tau')$ is the Fourier-space resistive Green's function defined in Eq. (7). The final step in computing $\eta_{ij}(\tau)$ is to use Eqs. (49) and (52) for the velocity spectrum tensor Π_{lm}.

The $\eta_{ij}(\tau)$ saturate at some constant values at late times; let us denote these constant values by $\eta_{ij}^\infty = \eta_{ij}(\tau\to\infty)$. If the mean magnetic field changes over times that are longer than the saturation time, we may use η_{ij}^∞ instead of the time-varying quantities $\eta_{ij}(\tau)$ in Eq. (55). Looking for solutions $\boldsymbol{B} \propto \exp[\lambda\tau + \mathrm{i}K_3X_3]$, we obtain the dispersion relation

$$\frac{\lambda_\pm}{\eta_T\,K_3^2} = -1 \pm \frac{1}{\eta_T}\sqrt{\eta_{21}^\infty\left(\frac{S}{K_3^2} + \eta_{12}^\infty\right) + \epsilon^2} \tag{58}$$

given in [5], where the new constants are defined as

$$\eta_t = \tfrac{1}{2}(\eta_{11}^\infty + \eta_{22}^\infty), \quad \eta_T = \eta + \eta_t, \quad \epsilon = \tfrac{1}{2}(\eta_{11}^\infty - \eta_{22}^\infty). \tag{59}$$

Exponentially growing solutions for the mean magnetic field are obtained when the radicand in Eq. (58) is both positive and exceeds η_T^2.

From Eqs. (57), (7), (49), and (52), it can be verified that the saturated values of the magnetic diffusivities, η_{ij}^∞, have the following general functional form:

$$\eta_{ij}^\infty = \eta_T\mathrm{Re}^2\frac{f_{ij}(S_h\mathrm{Re},\mathrm{Pr})}{1 + \chi(S_h,\mathrm{Re},\mathrm{Pr})}\,, \tag{60}$$

where the f_{ij} are dimensionless functions of two variables, and μ is a dimensionless function of three variables. Figures 1–3 display plots of η_t, η_{12}^∞, and η_{21}^∞ versus the dimensionless parameter $(-S_h\mathrm{Re})$. The scalings of the ordinates have been chosen for compatibility with the functional form displayed in Eq. (60). These plots should be compared with Fig. 3 of [5]. However, it should be noted that we operate in quite different parameter regimes: We are able to explore larger values of $|S_h|$, whereas [5] have done simulations for larger Re and Rm. The plots in Figs. 1(a)–1(c) are for Pr = 1, but for two sets of values of the Reynolds numbers: Re = Rm = 0.1, and Re = Rm = 0.5. Figures 2(a)–2(c) are for Re = 0.1 and Rm = 0.5, corresponding to Pr = 5. Figures 3(a)–3(c) are for Re = 0.5 and Rm = 0.1, corresponding to Pr = 0.2. As may be seen from Eq. (60), the ratio $(\eta_{12}^\infty/\eta_{21}^\infty)$ is a function

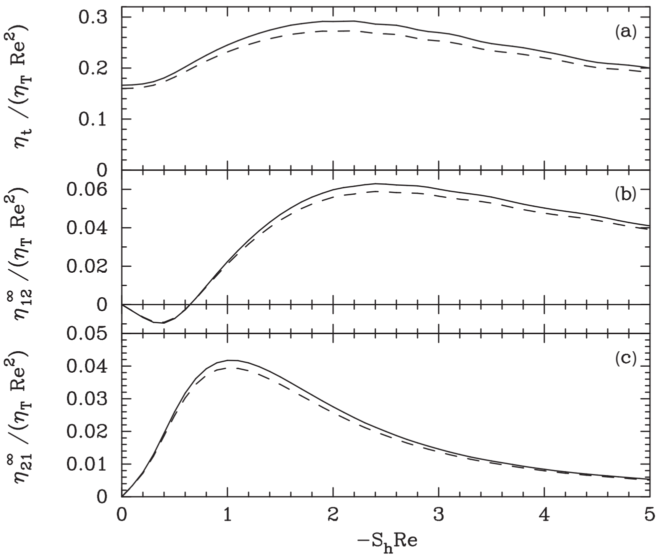

FIG. 1. Plots of the saturated quantities η_t, η_{12}^{∞}, and η_{21}^{∞} for Re = Rm = 0.1 and Re = Rm = 0.5, corresponding to Pr = 1, versus the dimensionless parameter ($-S_h$Re). The bold lines are for Re = Rm = 0.1, and the dashed lines are for Re = Rm = 0.5.

only of the two dimensionless parameters, (S_hRe) and Pr. In Fig. 4 we plot this ratio versus ($-S_h$Re) for all the cases considered in Figs. 1–3. Some noteworthy properties are as follows:

(1) We see that η_t is always positive. For a fixed value of ($-S_h$Re), the quantity $\eta_t/(\eta_T \mathrm{Re}^2)$ increases with Pr, and for a fixed value of Pr, it increases as ($-S_h$Re) increases from zero (which is consistent with [5]), attains a maximum value near ($-S_h$Re) ≈ 2, and then decreases while always remaining positive.

(2) As expected, the behavior of η_{12}^{∞} is more complicated. It is zero for ($-S_h$Re) = 0, and becomes negative for not too large values of ($-S_h$Re). After reaching a minimum value, it

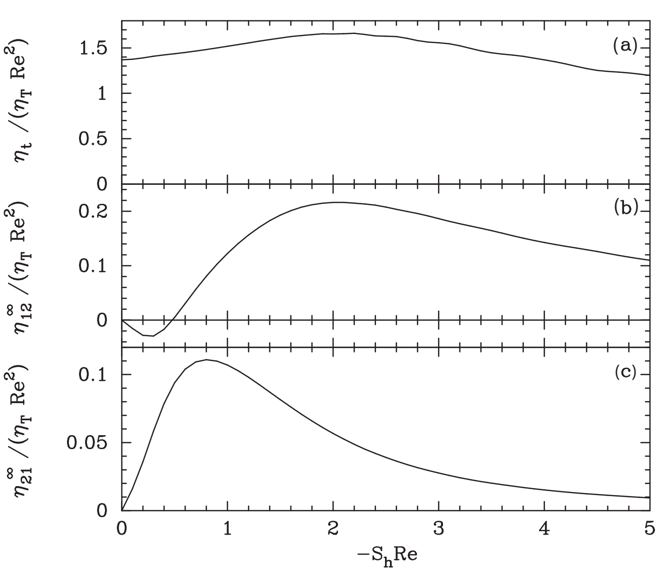

FIG. 2. Plots of the saturated quantities η_t, η_{12}^{∞}, and η_{21}^{∞} for Re = 0.1 and Rm = 0.5, corresponding to Pr = 5, versus the dimensionless parameter ($-S_h$Re).

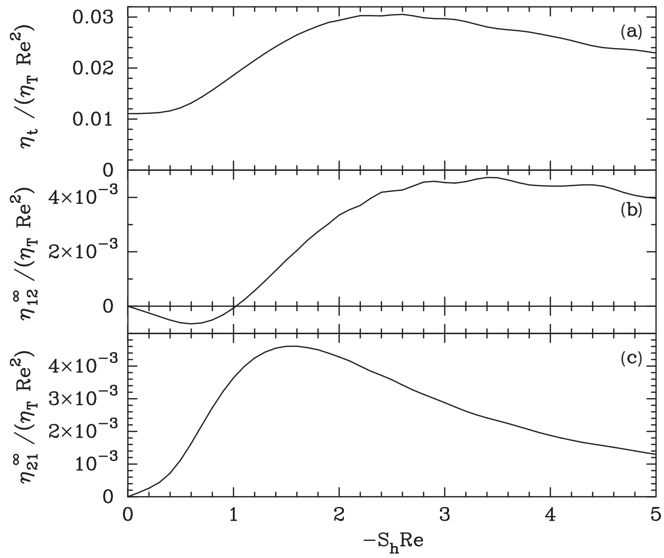

FIG. 3. Plots of the saturated quantities η_t, η_{12}^{∞}, and η_{21}^{∞} for Re = 0.5 and Rm = 0.1, corresponding to Pr = 0.2, versus the dimensionless parameter ($-S_h$Re).

then becomes an increasing function of ($-S_h$Re) and attains positive values for large ($-S_h$Re). Thus the sign of η_{12}^{∞} is sensitive to the values of the control parameters. This may help reconcile, to some extent, the fact that different signs for η_{12}^{∞} are reported in [12] and [5].

(3) As may be seen, η_{21}^{∞} is always positive. This agrees with the result obtained in [5,11], and [12].

(4) At first sight η_{12}^{∞} and η_{21}^{∞} appear to have quite different behaviors. However, closer inspection reveals certain systematics: as Pr increases, the overall range of values increases, while their shapes shift leftward to smaller values of ($-S_h$Re). From Eq. (60), it is clear that the ratio ($\eta_{12}^{\infty}/\eta_{21}^{\infty}$) is a function

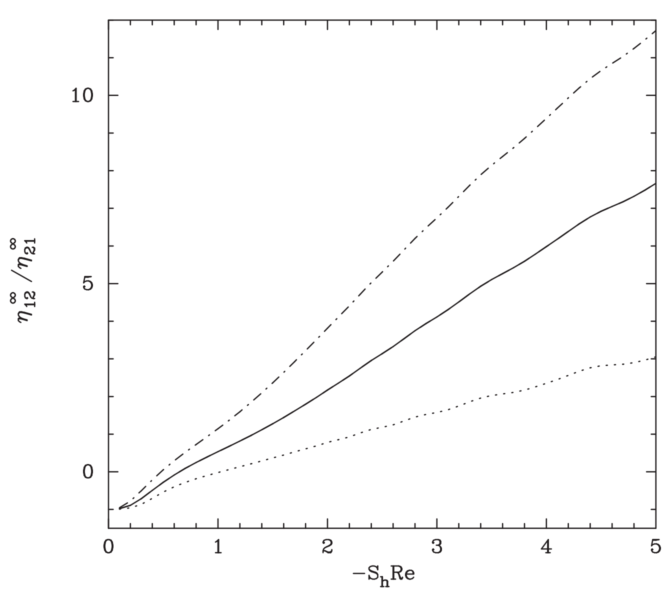

FIG. 4. Plots of the ratio ($\eta_{12}^{\infty}/\eta_{21}^{\infty}$) versus the dimensionless parameter ($-S_h$Re) for all the cases considered in Figs. 1–3. The bold line is for the two cases corresponding to Pr = 1, the dashed-dotted line is for Pr = 5, and the dotted line is for Pr = 0.2.

only of the two variables (S_hRe) and Pr. As Fig. 4 shows, this ratio is nearly a linear function of (S_hRe), whose slope increases with Pr.

(5) The magnitude of the quantity $\chi(S_h,\mathrm{Re},\mathrm{Pr})$ that appears in Eq. (60) is much smaller than unity. So $\eta_t/(\eta_T \mathrm{Re}^2)$, $\eta_{12}^{\infty}/(\eta_T \mathrm{Re}^2)$, and $\eta_{21}^{\infty}/(\eta_T \mathrm{Re}^2)$ can be thought of (approximately) as functions of ($-S_h$Re) and Pr. This is the reason why in Fig. 1 the bold and dashed lines lie very nearly on top of each other.

B. Implications for dynamo action and the shear-current effect

The mean magnetic field has a growing mode if the roots of Eq. (58) have a positive real part. It is clear that the real part of λ_- is always negative. So, for the growth of the mean magnetic field, the real part of λ_+ must be positive. Requiring this, we see from Eq. (58) that the condition for dynamo action is

$$\frac{\eta_{21}^{\infty} S}{\eta_T^2 K_3^2} + \frac{\eta_{12}^{\infty}\eta_{21}^{\infty}}{\eta_T^2} + \frac{\epsilon^2}{\eta_T^2} > 1. \tag{61}$$

In Fig. 5 we plot the last two terms, $(\eta_{12}^{\infty}\eta_{21}^{\infty}/\eta_T^2)$ and (ϵ^2/η_T^2), as functions of ($-S_h$Re), for all four cases: Re = Rm = 0.1; Re = Rm = 0.5; Re = 0.1,Rm = 0.5; and Re = 0.5,Rm = 0.1. As may be seen, the magnitudes of both terms are much smaller than unity, so they are almost irrelevant for dynamo action. Hence, there is growth of the mean magnetic field only when the first term $(\eta_{21}^{\infty} S/\eta_T^2 K_3^2)$ exceeds unity. This is possible for small enough K_3^2, so long as $(\eta_{21}^{\infty} S)$ is positive. However, we see from Figs. 1–3 that η_{21}^{∞} is always positive, implying that the product $(\eta_{21}^{\infty} S)$ is always negative. Therefore the inequality of (61) cannot be satisfied, and the mean-magnetic field always decays, a conclusion which is

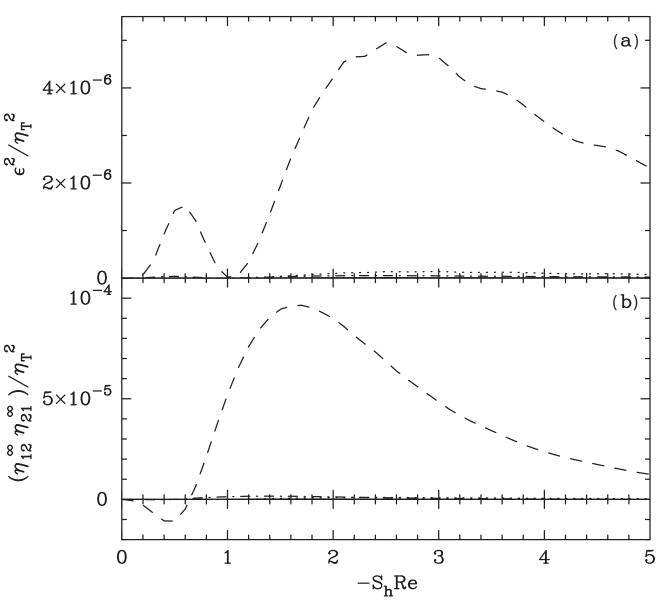

FIG. 5. Plots of (ϵ^2/η_T^2) and $(\eta_{12}^{\infty}\eta_{21}^{\infty}/\eta_T^2)$ versus the dimensionless parameter ($-S_h$Re) for all four cases considered in Figs. 1–3. The bold lines are for Re = Rm = 0.1; the dashed lines are for Re = Rm = 0.5; the dashed-dotted lines are for Re = 0.1,Rm = 0.5; and the dotted lines are for Re = 0.5,Rm = 0.1.

in agreement with those of [5,11,12]. We can understand the above results more physically. Let us assume that $|K_3|$ is small enough, and keep only the most important terms in Eq. (55). Then we have

$$\frac{\partial B_1}{\partial \tau} = -\eta_{21}^{\infty}\frac{\partial^2 B_2}{\partial X_3^2} + \cdots, \quad \frac{\partial B_2}{\partial \tau} = S B_1 + \cdots, \tag{62}$$

where we have used the saturated values of the magnetic diffusivity. If we now look for modes of the form $\boldsymbol{B} \propto \exp[\lambda\tau + \mathrm{i}K_3 X_3]$, we obtain the dispersion relation, $\lambda_\pm = \pm K_3\sqrt{\eta_{21}^{\infty} S}$. So it is immediately obvious that λ_+ is real and positive—i.e., the mean magnetic field grows—only when the product $(\eta_{21}^{\infty} S)$ is positive. However, this product happens to be negative, and the mean magnetic field is a decaying wave.

The above results have direct bearing on the *shear-current effect* [10]. This effect refers to an extra contribution to the mean EMF which is perpendicular to both the mean vorticity (of the background shear flow) and the mean current. From Eq. (53) we see that in our case, the relevant term is the contribution $-\eta_{21}^{\infty} J_1$ to $\mathcal{E}_2$. As Figs. 1–3 show, the diffusivity η_{21}^{∞} is nonzero only in the presence of shear, so the word *shear* refers to this. The word *current* refers to J_1, the cross-field component of the electric current associated with the mean magnetic field.[1] The shear-current effect would lead to the growth of the mean magnetic field (for small enough K_3), if only the product $(\eta_{21}^{\infty} S)$ is positive. However, as we have demonstrated, this product is negative, so the shear-current effect cannot be responsible for dynamo action, at least for small Re and Rm, but for all values of the shear parameter.

V. CONCLUSIONS

Building on the formulation of [14], we have developed a theory of the *shear dynamo problem* for small magnetic and fluid Reynolds numbers, but for arbitrary values of the shear parameter. Our primary goal is to derive precise analytic results which can serve as benchmarks for comparisons with numerical simulations. A related goal is to resolve the controversy surrounding the nature of the shear-current effect, without treating the shear as a small parameter. We began with the expression for the Galilean-invariant mean EMF derived in [14], and specialized to the case of a mean magnetic field that is slowly varying in time. This resulted in the simplification of the mean-field induction equation, from an integrodifferential equation to a partial differential equation. This reduction is the first step to the later comparison with the numerical experiments of [5]. Explicit expressions for the transport coefficients α_{il} and η_{iml} were derived in terms of the two-point velocity correlators which, using results from [14], were then expressed in terms of the velocity spectrum tensor. Then we proved that when the velocity field is nonhelical,

[1]Shear also makes an additional contribution through the SB_1 contribution to $(\partial B_2/\partial\tau)$, which accounts for the product $(\eta_{21}^{\infty} S)$ playing an important role. However, this is just the well-known physical effect of the shearing of the cross-shear component of the mean magnetic field to generate a shearwise component; it does not have any bearing on the word *shear* in the phrase *shear-current effect*.

the transport coefficient α_{il} vanishes; just like everything else in this paper, this result is nonperturbative in the shear parameter. We then considered forced, stochastic dynamics for the incompressible velocity field at low Reynolds number. An exact, explicit solution for the velocity field was derived, and the velocity spectrum tensor was calculated in terms of the Galilean-invariant forcing statistics. For nonhelical forcing, the velocity field is also nonhelical and the transport coefficient α_{il} vanishes, as noted above. We then specialized to the case when the forcing is not only nonhelical, but isotropic and delta correlated in time as well. We considered the case when the mean field was a function only of the spatial coordinate X_3 and time τ; the purpose of this simplification was to facilitate comparison with the numerical experiments of [5]. Explicit expressions were derived for all four components, $\eta_{11}(\tau)$, $\eta_{22}(\tau)$, $\eta_{12}(\tau)$, and $\eta_{21}(\tau)$, of the magnetic diffusivity tensor, in terms of the velocity spectrum tensor. Important properties of this fundamental object are as follows:

(1) All the components of η_{ij} are zero at $\tau = 0$ and saturate at finite values at late times, which we denote by η_{ij}^{∞}.

(2) The off-diagonal components, η_{12} and η_{21}, vanish when the microscopic resistivity vanishes.

(3) The sign of η_{12}^{∞} is sensitive to the values of the control parameters. This may help reconcile, to some extent, the fact that different signs for η_{12}^{∞} are reported in [12] and [5].

We derived the condition—the inequality (61)—required for the growth of the mean magnetic field: The sum of three terms must exceed unity. It was demonstrated that two of the terms are very small in magnitude, and hence dynamo action was controlled by the behavior of one term. That is, the mean magnetic field would grow if $(\eta_{21}^{\infty} S/\eta_T^2 K_3^2)$ exceeds unity. This is possible for small enough K_3^2, so long as $(\eta_{21}^{\infty} S)$ is positive. However, we see from Figs. 1–3 that η_{21}^{∞} is always positive, implying that the product $(\eta_{21}^{\infty} S)$ is always negative. Thus the mean magnetic field always decays, a conclusion which is in agreement with those of [5,11,12]. We then related the above conclusions to the shear-current effect, and demonstrated that the shear-current effect cannot be responsible for dynamo action, at least for small Re and Rm, but for all values of the shear parameter. In [5], it is suggested that the dynamo action observed in their numerical experiments might be due to a fluctuating α effect; addressing this issue is the scope of our present calculations.

[1] H. K. Moffatt, *Magnetic Field Generation in Electrically Conducting Fluids* (Cambridge University Press, Cambridge, 1978).

[2] F. Krause and K.-H. Rädler, *Mean-Field Magnetohydrodynamics and Dynamo Theory* (Pergamon Press, Oxford, 1980).

[3] A. Brandenburg and K. Subramanian, Phys. Rep. **417**, 1 (2005).

[4] N. Leprovost and E.-j. Kim, Astrophys. J. **696**, L125 (2009).

[5] A. Brandenburg, K.-H. Rädler, M. Rheinhardt, and P. J. Käpylä, Astrophys. J. **676**, 740 (2008).

[6] T. A. Yousef, T. Heinemann, A. A. Schekochihin, N. Kleeorin, I. Rogachevskii, A. B. Iskakov, S. C. Cowley, and J. C. McWilliams, Phys. Rev. Lett. **100**, 184501 (2008).

[7] T. A. Yousef, T. Heinemann, F. Rincon, A. A. Schekochihin, N. Kleeorin, I. Rogachevskii, S. C. Cowley, and J. C. McWilliams, Astron. Nachr. **329**, 737 (2008).

[8] P. J. Käpylä, M. J. Korpi, and A. Brandenburg, Astron. Astrophys. **491**, 353 (2008); **500**, 633 (2009).

[9] D. W. Hughes and M. R. E. Proctor, Phys. Rev. Lett. **102**, 044501 (2009).

[10] I. Rogachevskii and N. Kleeorin, Phys. Rev. E **68**, 036301 (2003); **70**, 046310 (2004); Astron. Nachr. **329**, 732 (2008).

[11] K.-H. Rädler and R. Stepanov, Phys. Rev. E **73**, 056311 (2006).

[12] G. Rüdiger and L. L. Kitchatinov, Astron. Nachr. **327**, 298 (2006).

[13] S. Sridhar and K. Subramanian, Phys. Rev. E **79**, 045305(R) (2009); **80**, 066315 (2009).

[14] S. Sridhar and N. K. Singh, J. Fluid Mech. **664**, 265 (2010).

[15] F. Krause and K.-H. Rädler, *Elektrodynamik der mittleren Felder in turbulenten leitenden Medien und Dynamotheorie, in Ergebnisse der Plasmaphysik und der Gaselektronik*, Band 2 (Akademie-Verlag, Berlin, 1971), pp. 2–154.